

1 **Disentangling fine-scale effects of environment on malaria detection and infection to design risk-**
2 **based disease surveillance systems in changing landscapes**

3

4 **Authors:** Kimberly M Fornace*^{1,2}, Ralph A Reyes³, Maria Lourdes M Macalinao³, Alison Paolo N Bareng³,
5 Jennifer S Luchavez³, Julius Clemence R Hafalla¹, Fe Esperanza J Espino³, Chris J Drakeley¹

6

7 1. Faculty of Infectious and Tropical Diseases, London School of Hygiene and Tropical Medicine,
8 Keppel Street, London WC1E 7HT, United Kingdom

9 2. Centre for Climate Change and Planetary Health, London School of Hygiene and Tropical
10 Medicine, Keppel Street, London WC1E 7HT, United Kingdom

11 3. Department of Parasitology, Research Institute for Tropical Medicine, 9002 Research Drive,
12 Alabang, Muntlupa, 1781 Metro Manila, Philippines

13

14

15

16 *** Corresponding author:**

17 Kimberly M Fornace

18 Kimberly.Fornace@lshtm.ac.uk

19 London School of Hygiene and Tropical Medicine

20 Keppel Street

21 London, WC1E 7HT, United Kingdom

22 +44 (0) 20 7927 2010

23

24

25 **Abstract:**

26

27 Landscape changes have complex effects on malaria transmission, disrupting social and
28 ecological systems determining the spatial distribution of risk. Within Southeast Asia, forested
29 landscapes are associated with both increased malaria transmission and reduced healthcare access.
30 Here, we adapt an ecological modelling framework to identify how local environmental factors influence
31 the spatial distributions of malaria infections, diagnostic sensitivity and detection probabilities in the
32 Philippines. Using convenience sampling of health facility attendees and Bayesian latent process models,
33 we demonstrate how risk-based surveillance incorporating forest data increases the probability of
34 detecting malaria foci over three-fold and enables estimation of underlying distributions of malaria
35 infections. We show the sensitivity of routine diagnostics varies spatially, with the decreased sensitivity
36 in closed canopy forest areas limiting the utility of passive reporting to identify spatial patterns of
37 transmission. By adjusting for diagnostic sensitivity and targeting spatial coverage of health systems, we
38 develop a model approach for how to use landscape data within disease surveillance systems. Together,
39 this illustrates the essential role of environmental data in designing risk-based surveillance to provide an
40 operationally feasible and cost-effective method to characterise malaria transmission while accounting
41 for imperfect detection.

42

43 **Background:**

44

45 Malaria transmission is highly variable spatially, driven by the geographical distribution of human
46 populations, mosquito vectors and the environments in which these populations interact (1).
47 Surveillance systems aim to identify these high-risk locations and populations in order to effectively
48 plan, implement and evaluate control policies and measures. As control programmes reduce incidence

49 and transmission decreases, spatial heterogeneity becomes more pronounced, necessitating
50 increasingly higher resolution data to detect foci of infection (2). This becomes increasingly critical in
51 rapidly changing environments, where changing human populations and vector habitats may cause
52 significant shifts in transmission patterns (3). However, despite extensive research linking landscape
53 with malaria transmission, landcover data rarely informs malaria surveillance systems.

54

55 For passive surveillance systems relying on reported malaria case data, understanding spatial
56 distributions of risk is further challenged by underreporting due to health-seeking behaviour or
57 asymptomatic infections present in the community. Increasing evidence suggests the proportion of
58 asymptomatic malaria infections not detectable by standard diagnostics increases in low transmission
59 settings, resulting in large numbers of infections not detected by passive surveillance systems (4, 5).
60 These asymptomatic infections are commonly seen in older age groups, with potentially different risk
61 factors and spatial distributions from clinical malaria cases (6, 7). Population-based community surveys
62 remain the gold standard for assessing spatial patterns of infection; however, these sampling
63 approaches are highly resource intensive and may require very large sample sizes in low transmission
64 settings. Alternatively, more operationally feasible surveys of easy access groups, such as health facility
65 attendees or school children, are used to increase probability of detecting infections within the
66 community (e.g. (8-11)). However, both approaches targeting clinical cases and easy access groups are
67 inherently biased and do not fully capture the spatial distribution of infections.

68

69 Within ecology, estimates of species distribution or abundance are similarly challenged by imperfect
70 detection and spatially biased observation processes (12). Occupancy models are widely used to
71 estimate the probability that a species occupies a geographic location within a specified time period
72 while accounting for possible non-detection (13). This method partitions observation processes

73 determining detection probability and biological processes determining occupancy probability, each
74 associated with potentially overlapping spatial and environmental covariates. This makes the simple
75 assumption that a species cannot be detected if it is not present; however, if present, the species may or
76 may not be detected during sampling. In addition to allowing estimation of true occupancy states as a
77 latent variable, this method allows quantification of uncertainty in the observation process under
78 different sampling scenarios (14-16).

79

80 Here, we combine occupancy models with practical health facility surveys and molecular
81 diagnostics to evaluate the spatial coverage of surveillance approaches and their ability to detect
82 locations with recent malaria transmission. By estimating a spatially explicit sensitivity of different
83 diagnostic methods, we illustrate how environmental data can be used to develop operationally feasible
84 risk-based surveillance systems to increase the probability of detecting areas of infection while
85 rationalising scarce resources. This provides an adaptable framework to integrate convenience sampling
86 approaches into existing disease surveillance systems to target control measures and characterise
87 spatial and environmental drivers of infection from opportunistically collected data.

88

89 Using rolling cross-sectional health facility-based surveys in which all attendees regardless of
90 patient status or symptoms were screened for malaria using routine and molecular diagnostics, with
91 residences geolocated in real-time using tablet-based applications, we apply this approach to describe
92 the spatial distribution of malaria infections in Rizal, Palawan, The Philippines (Figure 1 (11)). While the
93 Philippines has made substantial progress towards malaria elimination, with 50 provinces declared
94 malaria free, Palawan contributes over 95% of malaria cases nationally, including 2718 cases from the
95 municipality of Rizal in 2018 (17). Deforestation rates have increased markedly within Rizal; of the 24%
96 decrease in forest cover between 2000 – 2018, over 50% of deforestation occurred after 2015, largely

97 driven by agricultural expansion (18). Within this region, malaria risks are strongly associated with
98 proximity to forested areas due to both vector ecology and occupational risks (19). Described as
99 “frontier malaria,” factors associated with increased malaria risks, such as proximity to forest edges and
100 recent deforestation, are also associated with reduced healthcare access, resulting in potentially
101 complex interactions between detection bias and infection risks (20).

102
103 Our results illustrate that enhanced health facility-based surveys increase the probability of
104 detecting locations with malaria infections by markedly increasing the spatial coverage of the
105 surveillance system in addition to simply increasing the numbers of individuals screened. By comparing
106 locations of infections detected by routine diagnostics (microscopy and/ or rapid diagnostic tests (RDTs))
107 with sub-patent infections only detectable by molecular methods, we show the sensitivity of routine
108 diagnostics decreases in highly forested areas, with many locations of malaria transmission only
109 detectable by molecular methods. We demonstrate how these findings can be used to develop
110 operationally feasible and cost-effective environmentally targeted risk-based surveillance methods and
111 prioritise locations with high probabilities of infection not captured by existing surveillance systems.

112

113 **Figure 1.** Study area and forest cover in 2017

114

115

116 **Results:**

117

118 *Impact of survey method on detection probability*

119

120 We conducted monthly rolling cross-sectional surveys at 27 health facilities across Rizal,
121 Palawan over a one-year period (Figure S1). All consenting individuals, regardless of symptoms or

122 patient status, were screened for malaria using microscopy or RDTs and polymerase chain reaction (PCR)
123 as described by (21). As multiple malaria species are present in this area and over 75% of infections were
124 with *Plasmodium falciparum*, we classified malaria as positive for any *Plasmodium* species. Using this
125 data, we initially compared two surveillance approaches: 1. Standard - passive case detection (PCD),
126 including febrile patients screened using routine diagnostics (RDTs or microscopy) as per current
127 national surveillance guidelines; 2. Enhanced – standard PCD plus screening all health facility attendees
128 with both routine and molecular methods.

129

130 Between June 2016 – June 2017, 5767 individuals were enrolled in this study, including 1914
131 (33.2%) febrile patients screened for malaria by existing passive surveillance systems (21). Of these, 801
132 individuals (13.9%) were positive for malaria by molecular methods and 498 were positive by RDT or
133 microscopy. We geolocated all residences in Rizal (n=7313), identifying individuals screened by PCD from
134 698 unique locations while enhanced surveillance screened individuals from 2201 locations (Table S2).
135 Malaria infections were detected at 352 household locations using enhanced surveillance and 117
136 locations by standard PCD.

137

138 As control measures are targeted based on reported locations with malaria infection and over
139 80% of infected locations had only one infected individual detected, we chose to model whether malaria
140 infection was present or absent in a specific location (occupancy) rather than incidence. Detection
141 probabilities, the probability of screening at least one individual from a location during the study period,
142 varied geographically, with travel time to the nearest health facility negatively associated with detection
143 probability by both PCD and enhanced surveillance methods (Table 1). Enhanced surveillance increased
144 detection probabilities over three-fold compared to standard PCD (mean probability 3.34, 95%BCI: 1.03

145 – 8.27) in addition to markedly increasing spatial coverage of surveillance, particularly in rural
146 populations living in forested areas (Figure 2A, 2B).

147

148 **Figure 2.** Posterior probability of infection under different sampling scenarios adjusted for detection
149 probabilities: A. detection probability using routine passive case detection; B. detection probability using
150 health facility-based surveys; C. probability of infection estimated from passive case detection using
151 routine diagnostics; D. probability of infection estimated from active case detection using molecular
152 diagnostics

153

154

155

156

157

158

159 *Spatial distribution of infection*

160

161 Incorporating these detection probabilities into hierarchical occupancy models revealed a much
162 wider spatial distribution of malaria detected by enhanced surveillance compared to PCD alone,
163 identifying areas of infection not captured by existing surveillance systems (Figure 2C, 2D). We identified
164 a range of differing spatial and environmental risk factors for infections detected by different diagnostic
165 methods; however, all infections were associated with proximity to closed canopy forests in more rural
166 populations (Table 1). For joint models for each surveillance scenario, incorporating a shared spatial
167 random effect between detection and infection probability improved model performance, suggesting a
168 common spatial process driving healthcare access and disease risks (Table S3).

169

170 **Table 1.** Posterior estimates of fixed effects and spatial range for joint models of A. standard PCD and B.
 171 enhanced surveillance

172
 173 A.

	Mean	SD	95% BCI
Probability of detection			
Distance to roads	0.226	0.125	-0.020, 0.227
Travel time to clinic	-0.317	0.120	-0.561, -0.090
Distance to forest	-0.112	0.053	-0.217, -0.009
Spatial range (km)	8.140	2.500	4.319, 14.050
Probability of infection			
Distance from roads	0.094	0.101	-0.109, 0.287
Population density	-0.603	0.145	-0.894, -0.322
Precipitation of wetness month	0.212	0.107	-0.006, 0.420
Distance from closed canopy forest	-0.222	0.156	-0.537, 0.078
Spatial range (km)	1.752	1.096	0.493, 4.643
Scaling parameter for shared spatial effect	0.590	0.163	0.282, 0.921

174 ** All covariates mean-centred and scaled

175
 176 B.

	Mean	SD	95% BCI
Probability of detection			
Population density	-0.533	0.085	-0.701, -0.368
Travel time to clinic	-0.511	0.107	-0.729, -0.309
Aspect	0.094	0.039	0.017, 0.171
Spatial range (km)	15.804	6.130	7.212, 30.957
Probability of infection			
Distance from roads	0.285	0.071	0.145, 0.423
Upslope area	0.181	0.111	-0.038, 0.399
Topographic wetness index	-0.243	0.120	-0.481, -0.011
Temperature annual range	0.236	0.098	0.043, 0.428
Distance from closed canopy forest	-0.326	0.111	-0.548, -0.112
Spatial range (km)	0.897	0.232	0.532, 1.438
Scaling parameter for shared spatial effect	1.216	0.177	0.887, 1.179

177 ** All covariates mean-centred and scaled

178
 179

180 To explore the factors determining these differing distributions of infections, we estimated the
 181 probability of patent malaria detectable by RDT or microscopy in all malaria infections we identified.
 182 Malaria infected individuals were identified from 435 locations and over one third of infected individuals
 183 (37.8%, 95% CI: 34.5-41.3%) could only be detected by molecular methods. Subpatent malaria was
 184 substantially more common in forested areas with the odds of patent infections increasing 1.23 (95%BCI

185 1.03-1.47) with every kilometre distant from closed canopy forested areas (Table 2). Using data from all
186 residence locations identified within Rizal, we predicted a location-specific probability of patent malaria,
187 equivalent to the sensitivity of routine diagnostics (RDT and/or microscopy) (Figure S2).

188

189 **Table 2.** Posterior estimates of fixed effects for malaria positive households detected by routine
190 diagnostics (RDT and microscopy) compared to molecular methods

	Mean	SD	95% BCI
Distance from closed canopy forest*	0.225	0.112	0.036, 0.476
Annual precipitation*	-0.318	0.121	-0.620, -0.145
Precipitation of wettest month*	0.256	0.085	0.091, 0.422
Population density ^{2*}	0.093	0.087	-0.078, 0.263

191 * Mean-centred and scaled

192

193 *Evaluating surveillance systems*

194

195 As our primary aim was to identify all locations of malaria infection, we evaluated surveillance
196 approaches against estimates of true infection status using molecular diagnostics and all available
197 spatial data. Accounting for spatial bias of collection data, we estimated 11.4% (95%BCI: 4.6%-21.9%) of
198 all locations in Rizal had malaria infections during the sampling period. While no surveillance method
199 identified all areas of infection perfectly, enhanced surveillance using molecular methods identified
200 38.7% (95% BCI: 33.6-43.8%) of infected locations while PCD only identified 5.7% (95% BCI: 0.1 – 11.9%).
201 Including molecular diagnostics in PCD only slightly improved the probability of detecting infections
202 while conducting health facilities using only routine diagnostics increased the number of infected
203 locations identified slightly more (Figure 3A, Figure S4). We additionally identified 247 locations with a
204 very low (<0.05% probability) of detection by any health facility-based surveillance.

205

206 Based on distributions of malaria infections and probability of detection by routine diagnostics,
207 we additionally explored the use of environmentally-stratified risk-based surveillance approaches. We

208 defined high-risk areas based on distances from closed canopy forest (Figure S3). Evaluating costs of
 209 each surveillance system relative to baseline costs of standard PCD (Methods, SI), we estimated the total
 210 cost per location with malaria infection identified (Figure 3B). As the cost per infection detected was
 211 most sensitive to inclusion of molecular diagnostics, we defined a risk-based surveillance approach using
 212 health facility surveys in all areas and only applying molecular diagnostics to locations within 100m of
 213 closed canopy forest areas (Table 3, Figure S5). This risk-based surveillance approach almost halved the
 214 cost of detecting a location of infection compared to enhanced surveillance, from USD 603.10 (95% BCI:
 215 530.02 – 690.82) to USD 370.00 (95% BCI: 313.18- 444.04) while detecting almost as many locations of
 216 infections.

217

218 **Table 3.** Surveillance methods assessed

219

	Survey method		Diagnostic method		Total cost (USD)
	Passive case detection	Health facility surveys	Routine (RDT/ microscopy)	Molecular	
1: Standard PCD	X		X		-
2: Enhanced surveillance	X	X	X	X	193,547.70
3: PCD + molecular	X		X	X	56,654.40
4: Health facility surveys + routine	X	X	X		22,844.50
5: Risk-based surveys + diagnostics	X	Risk zone only	X	Risk zone only	

220

221 **Figure 3.** Evaluation of surveillance methods described in Table 3 by A. estimated numbers of locations
 222 with malaria infections not detected, and B. estimated additional costs per location with malaria
 223 infections detected (relative to standard PCD)

224

225

226

227 Discussion

228

229 The spatial distribution of malaria is driven by a complex interplay of environmental and social
 230 factors influencing both disease transmission and identification by health systems. Statistical methods

231 enabling examination of processes driving infection and detection provide an invaluable tool to evaluate
232 the roles of environmental factors and develop targeted surveillance approaches. Here, we demonstrate
233 a convenience sampling approach using health facility surveys markedly increases spatial coverage of
234 surveillance systems; incorporating these surveys with satellite-derived remote sensing data allows
235 estimation of the underlying distribution of infection not captured by passive surveillance. We
236 additionally show higher proportions of subpatent malaria infections in forested areas, highlighting the
237 limited utility of routine diagnostics within these regions. Applying these findings, we develop a cost-
238 effective and operationally feasible risk-based surveillance approach using environmental data and
239 illustrate how landscape data can be incorporated into disease surveillance systems.

240

241 Despite extensive research identifying proximity to forests as risk factors for malaria infection in
242 Southeast Asia (e.g. (3, 22-27)), landscape data are not routinely used to design or inform surveillance
243 systems. Malaria control programmes typically conduct community-based active case detection in
244 response to reported malaria cases (2); however, we show this may miss a substantial proportion of
245 active malaria foci due to biases in health-seeking behaviour and increased prevalence of subpatent
246 malaria within higher transmission areas. Although mechanisms driving this relationship between forest
247 cover and subpatent malaria are not known, patent malaria infections are more common in children in
248 this area and settlements in closer proximity to forests may have different demographic compositions
249 (e.g. logging and plantation camps) (21). Previous studies have also suggested a role for immunity in
250 high transmission areas, with individuals repeatedly exposed to malaria commonly having lower parasite
251 densities (4). Despite lower parasite densities, these subpatent infections can lead to infections in
252 mosquitoes and may have a critical role in sustaining transmission in elimination settings, highlighting
253 the importance of identifying and treating these individuals (28).

254

255 While screening entire populations may be prohibitively costly and intensive, the increasing
256 availability of satellite-based remote sensing data provides new opportunities to use environmental data
257 to target surveillance activities (29). Surveillance systems for malaria, as well as for other low incidence
258 or emerging diseases, are challenged by the need to identify relatively rare events with shifting spatial
259 patterns. Widely used in veterinary epidemiology, risk-based surveillance uses known risk factors to
260 focus intensive surveillance activities on the populations where rare events are most likely to occur (30).
261 Integrating remote-sensing derived environmental data into this approach provides an adaptable
262 framework which can be easily updated in changing landscapes. Further, quantifying the detection
263 probabilities associated with these surveillance approaches allows estimation of biases in data and
264 identification of populations not captured by opportunistic sampling and can be used to plan active case
265 detection. For this example, using health facility surveys, this enables evaluation of spatial patterns of
266 health seeking behaviour as well as populations outside health system coverage. Screening all
267 individuals attending health facilities, including those accompanying patients or for nonfebrile illnesses,
268 vastly increases the spatial coverage of surveillance. The improved performance of models including a
269 common spatial term for both infection and detection suggests processes determining healthcare
270 coverage also influence infection risks, demonstrating the multiple utilities of measuring health seeking
271 behaviour in this context.

272

273 Within this study, remote sensing data was used not only as covariates but also to define the
274 populations at risk. The application of machine learning approaches to identify building footprints from
275 very high resolution satellite imagery has produced increasingly accurate estimates of household
276 distributions and allows estimation of spatial distribution of the populations (31). Development of
277 tablet-based methods including population data and satellite imagery enabled near real-time
278 identification of the residences of health facility attendees in a rural population with no formal

279 addresses and limited internet connectivity (11). These tools and datasets can be further expanded to
280 create accessible interfaces for local health workers to use environmental and spatial data and
281 incorporate risk-based decision pathways on screening procedures and diagnostic tests based on
282 household locations and travel history. This approach can also be easily modified to include multiple
283 diseases with different underlying environmental risk factors and updated to include new environmental
284 data, such as near real time deforestation alerts (32). Despite advances in using meteorological data to
285 forecast vector-borne disease epidemics, landscape data is rarely used operationally and may provide
286 more actionable information within rapidly changing environments. While we have focused on malaria,
287 this is additionally relevant for targeting risk-based surveillance of emerging diseases, such as by
288 detecting rare spillover events in changing habitats.

289

290 Despite the utility of these methods, there were several limitations to this study. As this study
291 was designed to identify spatial locations of malaria infections within the sampling year, we did not
292 explore temporal patterns of infection or health seeking behaviours. However, the modelling approach
293 used is easily extendable to incorporate dynamic state-space models of changes in infection over time
294 (12). If health facility surveys were collected over longer periods of time, this could additionally be
295 expanded to incorporate seasonally varying meteorological data to further refine risk stratifications.
296 While populations at risk were defined using multiple datasets, this is likely to have limited coverage of
297 highly mobile indigenous populations not residing in permanent structures. Future work could explore
298 the utility of satellite imagery to identify these populations, such as through monitoring of forest
299 disturbance or modelling movement patterns. Within this study, the numbers of infections with
300 different *Plasmodium* species precluded species-specific analyses. As all species are transmitted by the
301 same mosquito vectors, environmental risk factors are expected to be similar; however, future work
302 could examine differences between spatial distribution by malaria species. Additionally, while molecular

303 approaches for malaria are not easily applied in rural settings, new diagnostics, such as lateral flow
304 assays and serological tests, may facilitate point of contact testing in the future (33, 34).

305
306 Even with these limitations, this provides a novel and adaptable surveillance approach for
307 environmentally driven diseases and demonstrates the role of landscapes in driving malaria infection
308 and detection within this region. Incorporation of forest data enables identification of cost-effective risk-
309 based surveillance approaches which increase probabilities of detecting malaria infections and can be
310 applied to support elimination efforts. Additionally, the process-based ecological modelling method
311 used provides a flexible framework to quantify detection probabilities and estimate the true spatial
312 distribution of infection using biased data from convenience-based sampling approaches.

313

314 **Methods:**

315 *Survey approaches*

316

317 We conducted cross-sectional health facility-based surveys at 27 facilities, including at one
318 Regional Health Unit (RHU), 9 Barangay Health Stations (BHS) and 17 RDT centres based in community
319 health worker households, established to increase access to malaria diagnosis and treatment (Figure S1).
320 For one week every month between June 2016 – June 2017, all individuals attending the health facility,
321 regardless of symptoms or patient status, were asked to participate in this survey. For consenting
322 individuals, malaria status was assessed using either microscopy or rapid diagnostic tests (RDTs), with
323 finger-prick blood samples collected on Whatman 3MM filter paper for subsequent polymerase chain
324 reaction (PCR) (21). We classified malaria as positive for any *Plasmodium* species as 75% of identified
325 species were *P. falciparum* and all malaria species are transmitted by common vectors in this area.

326 Household locations were identified on offline maps and basic demographic information was recorded
327 using GeoODK on Android tablets (11).

328

329 *Spatial and environmental covariates*

330

331 To define the locations of all households within Rizal, we extracted information on household
332 structure locations from the Facebook High Resolution Settlement Layer, a 30m resolution satellite-
333 based remote sensing derived dataset on all inhabited structures (35). This dataset was combined with
334 all reported households identified by survey participants and geolocated households from the 2015
335 Philippine census (36). We resampled all datasets to 50m resolution and removed duplicate locations to
336 account for spatial resolution of datasets and inaccuracies of reported household locations. To estimate
337 detection probabilities, we classified households included by a surveillance scenario if one or more
338 individuals were sampled. Similarly, households were classified as infected if one or more individuals
339 were identified as infected by diagnostics used by the surveillance approach.

340

341 Plausible covariates used to model detection or infection probabilities were assembled (Table
342 S1). Handheld GPS devices (Garmin, USA) were used to record locations of all sampled clinics and roads
343 within the region. Travel time to the nearest sampled clinic was calculated as accumulated cost from
344 friction surfaces extracted from (37). Additional environmental and spatial covariates included
345 population density (38), Euclidean distance from roads and bioclimatic variables (39). Elevation and
346 topographic measures, including topographic wetness index (TWI), upslope area and aspect, were
347 calculated from the ASTER Global Digital Elevation Model (40). Forest cover was classified as over 50%
348 canopy cover based on (18) and Euclidean distance was calculated to the forest edge, recent
349 deforestation within the past year and historical deforestation within the previous five years. We

350 additionally included closed canopy forest, defined as canopy cover over 90% with a minimum area of
351 0.5ha (41).

352

353 *Occupancy modelling*

354

355 Covariates were extracted for all identified household locations and Pearson correlation analysis
356 was used to assess multicollinearity between variables. To select variables for inclusion, nonspatial
357 binomial generalised linear models were fit separately for detection probabilities and infection
358 probabilities for each surveillance scenario using backwards stepwise model selection with a five-point
359 threshold for improvement in deviance information criteria (DIC) to minimise overfitting (42). Residual
360 spatial autocorrelation was assessed using Moran's I and performance assessed by area under the
361 receiver operating curve (AUC). Weakly informative priors of Normal (0, 1/0.01) were used for all
362 intercepts and coefficients. All models were implemented in Integrated Nested Laplace (INLA), with
363 10,000 posterior samples generated from the approximated posterior distribution to include uncertainty
364 in these estimates (43). Final models had an AUC of 85% for both surveillance approaches.

365

366 We modelled the distribution of infections under each surveillance scenario separately using
367 occupancy models in which the probability of detecting an infection (y_i) in location i is dependent on the
368 probability of detection (p_i) and presence of infection (ω_i) (13), modelled as:

369

$$y_i \sim \begin{cases} 0, & \omega_i = 0 \\ \text{Bernoulli}(p_i), & \omega_i = 1 \end{cases}$$

370

371 Where the linear predictor determining the probability of detection is modelled as:

372

$$\text{logit}(p_i) = \alpha_0 + \mathbf{X}_i\boldsymbol{\alpha} + u_i$$

373

374 Where α_0 represents the intercept, $\mathbf{X}_i\boldsymbol{\alpha}$ represents a vector of covariate effects and u_i is the spatial
375 effect modelled as a Matern covariance function using the stochastic partial differential equations
376 approach to represent the spatial process by Gaussian Markov random fields as implemented in INLA
377 (43, 44). The process determining the true state of malaria presence ω is determined by the true
378 probability of infection ψ :

$$\omega_i \sim \text{Bernoulli}(\psi_i)$$

379

380 With the linear predictor for the Bernoulli model specified as:

381

$$\text{logit}(\psi_i) = \beta_0 + \mathbf{X}_i\boldsymbol{\beta} + \gamma_i + Zu_i$$

382

383 Where β_0 represents the intercept, $\mathbf{X}_i\boldsymbol{\beta}$ represents a vector of covariate effects and γ_i represents the
384 spatial effect, modelled as described above. As processes influencing probability of detection
385 (healthcare access) additionally may impact infection, we include a shared spatial component Zu_i with
386 scaling parameter Z (45).

387

388 *Patent malaria distribution*

389

390 To explore factors affecting the distribution of locations of patent malaria infections (detected
391 by RDT or microscopy) compared to all infections, we subset all malaria infected locations. For J_j malaria
392 infected individuals identified in each location, the number of patent infections observed (m_i) is
393 modelled as:

$$m_i \sim \text{Binomial}(J_i, s_i)$$

394

395 With the linear predictor determining the probability of patent infections (s_i) modelled as:

396

$$\text{logit}(s_i) = \kappa_0 + \mathbf{X}_i \boldsymbol{\kappa}$$

397

398 Where κ_0 represents the intercept and $\mathbf{X}_i \boldsymbol{\kappa}$ represents a vector of covariate effects. Using data from all

399 locations included in the study site, we then predicted a location specific sensitivity of routine

400 diagnostics. Based on these results, we used environmental data to define an area with higher

401 probabilities of malaria infections only detectable by molecular diagnostics.

402

403 *Evaluation of surveillance systems*

404

405 We modelled the true probability of infection from the infection process model using data from

406 all available diagnostics. To compare surveillance methods with different survey and diagnostic

407 methods, we estimated the number of infected locations not detected as:

$$\sum_{i=1}^i \omega_i(1 - p_i) + \omega_i p_i(1 - s_i)$$

408 Where p_i is the probability of detection using different survey methods and s_i represents diagnostic

409 sensitivity, with PCR considered the gold standard. We additionally included risk-based surveillance

410 methods, using health facility surveys and molecular diagnostics in high risk areas defined by proximity

411 to closed canopy forest. All derived quantities were estimated using 10,000 posterior samples.

412

413 To evaluate the cost effectiveness of different surveillance approaches, we estimated the
414 additional costs to health systems of including different survey and diagnostic approaches (Table S4).
415 This excluded capital costs and costs already covered by existing health systems (e.g. RDT and
416 microscopy diagnostics for febrile patients). Health facility survey costs included additional payments to
417 personnel, training, equipment, RDT and microscopy for non-febrile participants, sample collection and
418 molecular diagnostics for all attendees and salary for a technician to support data management and
419 sample analysis. The costs of molecular diagnostics included DNA extraction and PCR reagents, assuming
420 all DNA extraction was completed using Chelex with 10% of samples verified using a commercial Qiagen
421 kit. To account for varying numbers of samples screened from each location, we estimated the mean
422 cost of molecular diagnostics per location as the total cost of molecular diagnostics divided by the total
423 number of locations included. We evaluated these against the estimated number of locations correctly
424 identified as a measure of cost effectiveness. All analysis was completed in R statistical programming
425 language (v 3.6), with maps visualised in R or ArcGIS (ESRI, Redlands, USA).

426

427 *Ethics approval*

428 This study was approached by the Institutional Review Board of the Research Institute for Tropical
429 Medicine, Department of Health Philippines (IRB:2016-04) and the Research Ethics Committee of the
430 London School of Hygiene and Tropical Medicine (11597). Written informed consent was obtained from
431 all participants or parents or guardians and assent obtained from children under 18.

432

433 *Data availability*

434 Data is available upon reasonable request and with permission of ethics committees in the Philippines
435 and United Kingdom. All R code needed to conduct these analyses will be available at

436 <https://github.com/kfornace>

437

438

- 439 1. Lambin EF, Tran A, Vanwambeke SO, Linard C, & Soti V (2010) Pathogenic landscapes:
440 interactions between land, people, disease vectors, and their animal hosts. *International journal*
441 *of health geographics* 9:54.
- 442 2. World Health Organisation (2018) Malaria surveillance, monitoring and evaluation: a reference
443 manual. (World Health Organization, Geneva).
- 444 3. Yasuoka J & Levins R (2007) Impact of deforestation and agricultural development on
445 anopheline ecology and malaria epidemiology. *The American journal of tropical medicine and*
446 *hygiene* 76(3):450-460.
- 447 4. Okell LC, *et al.* (2012) Factors determining the occurrence of submicroscopic malaria infections
448 and their relevance for control. *Nature communications* 3:1237.
- 449 5. Okell LC, Ghani AC, Lyons E, & Drakeley CJ (2009) Submicroscopic infection in Plasmodium
450 falciparum-endemic populations: a systematic review and meta-analysis. *The Journal of*
451 *infectious diseases* 200(10):1509-1517.
- 452 6. Zhou G, Afrane YA, Malla S, Githeko AK, & Yan G (2015) Active case surveillance, passive case
453 surveillance and asymptomatic malaria parasite screening illustrate different age distribution,
454 spatial clustering and seasonality in western Kenya. *Malaria journal* 14(1):41.
- 455 7. Hsiang MS, *et al.* (2019) Active case-finding for malaria: A three-year national evaluation of
456 optimal approaches to detect infections and hotspots through reactive case detection in the low
457 transmission setting of Eswatini. *Clin Infect Dis*.
- 458 8. Ashton RA, *et al.* (2015) Geostatistical modeling of malaria endemicity using serological
459 indicators of exposure collected through school surveys. *The American journal of tropical*
460 *medicine and hygiene* 93(1):168-177.
- 461 9. Stevenson JC, *et al.* (2013) Reliability of school surveys in estimating geographic variation in
462 malaria transmission in the western Kenyan highlands. *PloS one* 8(10):e77641.
- 463 10. Stresman GH, *et al.* (2014) High levels of asymptomatic and subpatent Plasmodium falciparum
464 parasite carriage at health facilities in an area of heterogeneous malaria transmission intensity
465 in the Kenyan highlands. *The American journal of tropical medicine and hygiene* 91(6):1101-
466 1108.
- 467 11. Fornace KM, *et al.* (2018) Use of mobile technology-based participatory mapping approaches to
468 geolocate health facility attendees for disease surveillance in low resource settings.
469 *International journal of health geographics* 17(1):21.
- 470 12. Bailey LL, MacKenzie DI, & Nichols JD (2013) Advances and applications of occupancy models.
471 *Methods in Ecology and Evolution* 5(12):1269-1279.
- 472 13. Hobbs NT & Hooten MB (2015) *Bayesian Models: A Statistical Primer for Ecologists* (Princeton
473 University Press, New Jersey, USA).
- 474 14. Banks-Leite C, *et al.* (2014) Assessing the utility of statistical adjustments for imperfect detection
475 in tropical conservation science. *J. Appl. Ecol.* 51(4):849-859.
- 476 15. Nelli L, Ferguson HM, & Matthiopoulos J (2019) Achieving explanatory depth and spatial breadth
477 in infectious disease modelling: Integrating active and passive case surveillance. *Stat Methods*
478 *Med Res*:962280219856380.
- 479 16. Salvador LCM, Deason M, Enright J, Bessell PR, & Kao RR (2018) Risk-based strategies for
480 surveillance of tuberculosis infection in cattle for low-risk areas in England and Scotland.
481 *Epidemiol Infect* 146(1):107-118.
- 482 17. Epidemiology Bureau (2018) Malaria surveillance report. ed Health PDo (Manila).
- 483 18. Hansen MC, *et al.* (2013) High-resolution global maps of 21st-century forest cover change.
484 *Science* 342(6160):850-853.
- 485 19. DOH P, WHO, & UCSF (2014) Eliminating malaria: case-study 6, Progress towards subnational
486 elimination in the Philippines. (World Health Organisation, Geneva).

487 20. de Castro MC, Monte-Mor RL, Sawyer DO, & Singer BH (2006) Malaria risk on the Amazon
488 frontier. *Proceedings of the National Academy of Sciences of the United States of America*
489 103(7):2452-2457.

490 21. Reyes RA, *et al.* (submitted) Improved detection of malaria infection through enhanced health
491 facility surveys.

492 22. Sanann N, *et al.* (2019) Forest work and its implications for malaria elimination: a qualitative
493 study. *Malaria journal* 18(1):376.

494 23. Hasyim H, *et al.* (2018) Spatial modelling of malaria cases associated with environmental factors
495 in South Sumatra, Indonesia. *Malaria journal* 17(1):87.

496 24. Guerra CA, Snow RW, & Hay SI (2006) A global assessment of closed forests, deforestation and
497 malaria risk. *Annals of tropical medicine and parasitology* 100(3):189-204.

498 25. Fornace KM, *et al.* (2016) Association between Landscape Factors and Spatial Patterns of
499 Plasmodium knowlesi Infections in Sabah, Malaysia. *Emerging infectious diseases* 22(2):201-208.

500 26. Durnez L, *et al.* (2013) Outdoor malaria transmission in forested villages of Cambodia. *Malaria*
501 *journal* 12:329.

502 27. Cui L, *et al.* (2012) Malaria in the Greater Mekong Subregion: heterogeneity and complexity.
503 *Acta tropica* 121(3):227-239.

504 28. Slater HC, *et al.* (2019) The temporal dynamics and infectiousness of subpatent Plasmodium
505 falciparum infections in relation to parasite density. *Nature communications* 10(1):1433.

506 29. Hay SI, George DB, Moyes CL, & Brownstein JS (2013) Big data opportunities for global infectious
507 disease surveillance. *PLoS medicine* 10(4):e1001413.

508 30. Stark KD, *et al.* (2006) Concepts for risk-based surveillance in the field of veterinary medicine
509 and veterinary public health: review of current approaches. *BMC Health Serv. Res.* 6:20.

510 31. Tiecke TG, *et al.* (2017) Mapping the world population one building at a time. *ArXiv*
511 arXiv:1712.05839.

512 32. Hansen MC, *et al.* (2016) Humid tropical forest disturbance alerts using Landsat data.
513 *Environmental Research Letters* 11(3).

514 33. Landier J, *et al.* (2018) Operational Performance of a Plasmodium falciparum Ultrasensitive
515 Rapid Diagnostic Test for Detection of Asymptomatic Infections in Eastern Myanmar. *Journal of*
516 *clinical microbiology* 56(8).

517 34. Plucinski MM, *et al.* (2019) Assessing Performance of HRP2 Antigen Detection for Malaria
518 Diagnosis in Mozambique. *Journal of clinical microbiology* 57(9).

519 35. Facebook Connectivity Lab & Center for International Earth Science Information Network
520 (CIESIN) Columbia University (2016) High resolution settlement layer (HRSL). (CIESIN, Columbia
521 University, New York).

522 36. Philippine Statistics Authority (2016) Philippine Population Density (Based on the 2015 Census of
523 Population).

524 37. Weiss DJ, *et al.* (2018) A global map of travel time to cities to assess inequalities in accessibility
525 in 2015. *Nature* 553(7688):333-336.

526 38. Lloyd CT, Sorichetta A, & Tatem AJ (2017) High resolution global gridded data for use in
527 population studies. *Sci Data* 4:170001.

528 39. Fick SE & Hijmans RJ (2017) Worldclim 2: New 1-km spatial resolution climate surfaces for global
529 land areas. *International Journal of Climatology*.

530 40. Land Processes Distributed Active Archive Center (LP DAAC) (2015) Advanced Spaceborne
531 Thermal Emission and Reflection Radiometer Global Digital Elevation Model (ASTER GDEM)
532 Version 2. (NASA EOSDIS Land Processes DAAC, USGS Earth Resources Observatoion and Science
533 (EROS) Center, Sioux Falls, South Dakota).

- 534 41. ALOS-2/ALOS Science Project Earth Observation Research Center (EORC) (2017) Global PALSAR-
535 2/PALSAR/JERS-1 Mosaic and Forest/Non-Forest map. (Japan Aerospace Exploration Agency
536 (JAXA)).
- 537 42. Redding DW, Tiedt S, Lo Iacono G, Bett B, & Jones KE (2017) Spatial, seasonal and climatic
538 predictive models of Rift Valley fever disease across Africa. *Philosophical transactions of the*
539 *Royal Society of London. Series B, Biological sciences* 372(1725).
- 540 43. Rue H, Martino S, & Chopin N (2009) Approximate Bayesian inference for latent Gaussian
541 models by using integrated nested Laplace approximations. *Journal of the Royal Statistical*
542 *Society* 71(Part 2):319-392.
- 543 44. Lindgren F & Rue H (2015) Bayesian Spatial Modelling with R-INLA. *Journal of Statistical*
544 *Software* 63(19).
- 545 45. Martins TG, Simpson D, Lindgren F, & Rue H (2013) Bayesian computing with INLA: new
546 features. *Computational Statistics and Data Analysis* 67:68-83.

547

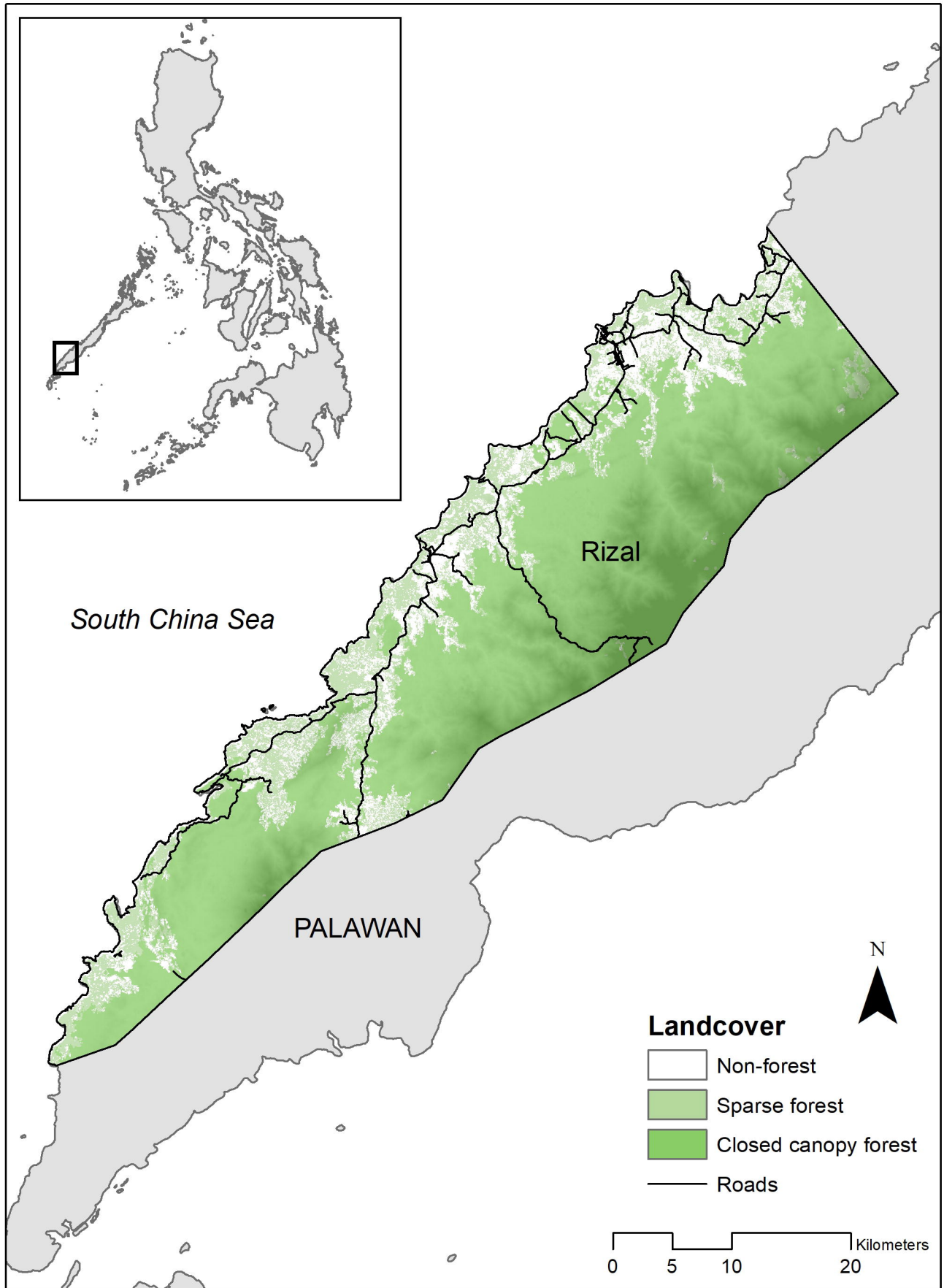
548 *Acknowledgements*

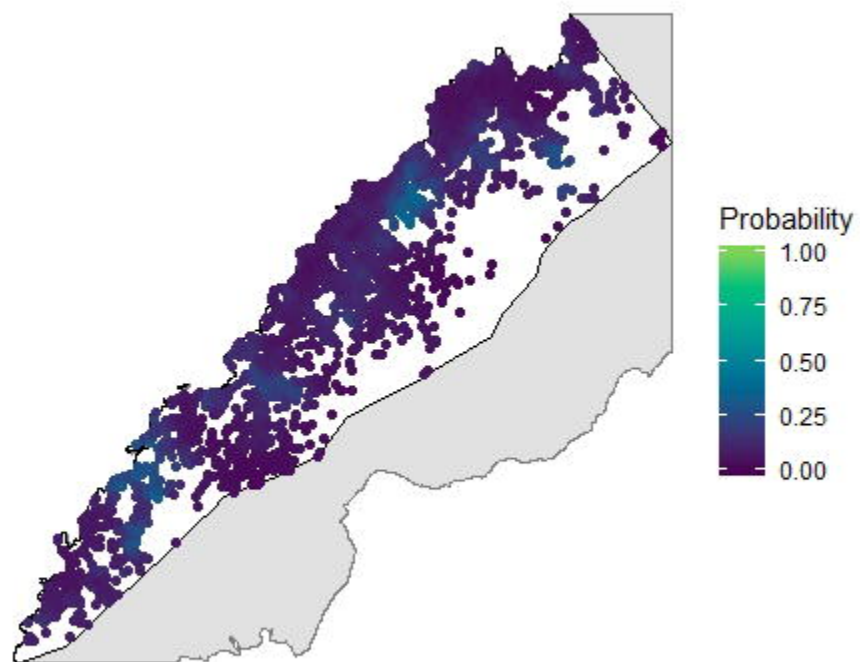
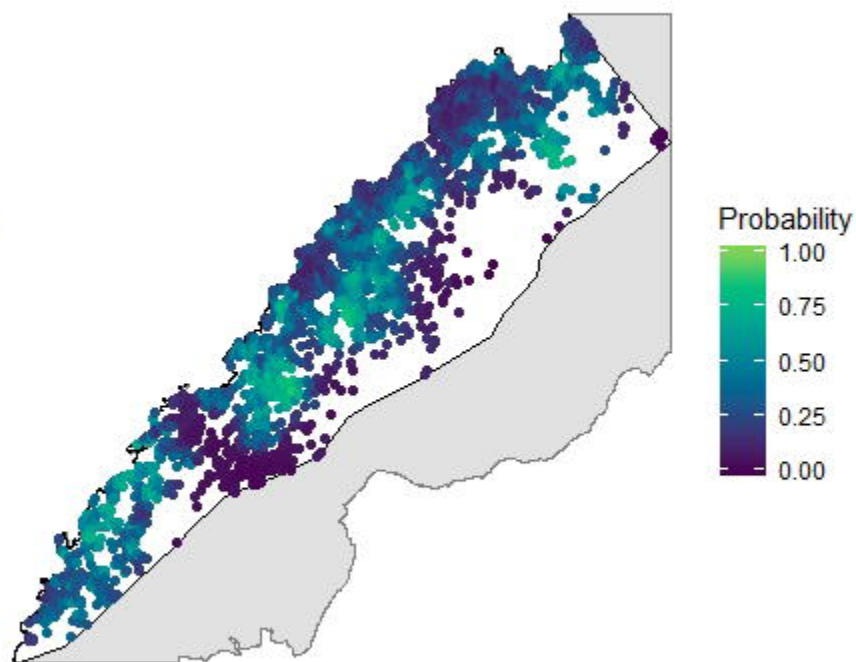
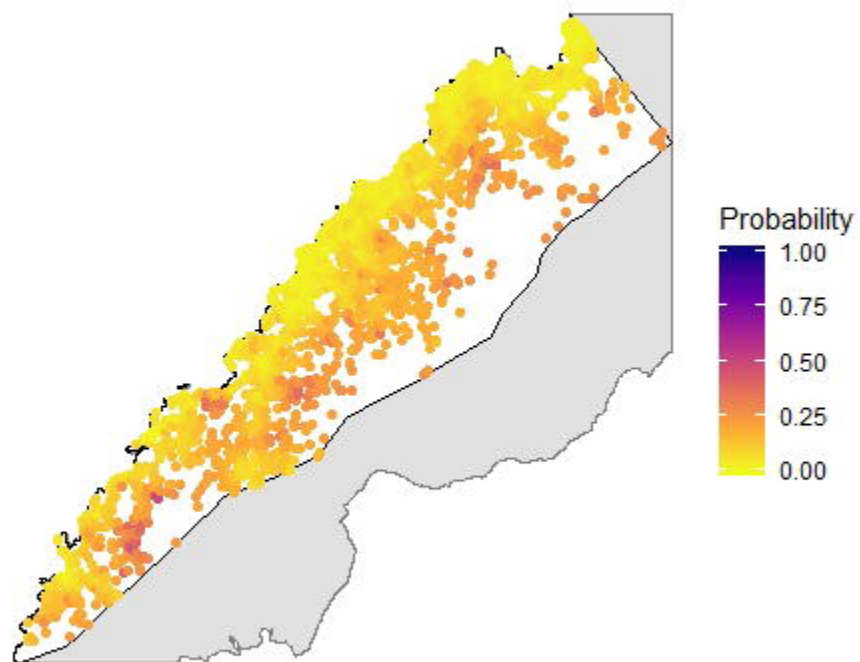
549 We would like to acknowledge the Newton Fund, Philippine Council for Health Research and
550 Development and UK Medical Research Council for funding received for ENSURE: Enhanced Surveillance
551 for control and elimination of malaria in the Philippines. We would additionally like to thank Ellaine de la
552 Fuente and Beulah Boncayo for supporting fieldwork as well as the local health staff and government of
553 Rizal, Palawan, the Philippines who supported this survey.

554

555 *Author contributions*

556 KMF, FE, JRCH and CJD designed this study. KMF analysed the data and wrote the manuscript. KMF and
557 RAR collected and analysed spatial and remote sensing data. RAR, MLMM, APNB and JSL collected the
558 health data and analysed samples. All authors read and approved the final manuscript.



A**B****C****D**